

USGS Award No. 04HQGR0071

INCORPORATING GEOTECHNICAL SITE RESPONSE INTO OPENSHA

Ellen M. Rathje, Ph.D., P.E.

University of Texas at Austin

ECJ 9.227, C1792

Austin, TX 78712

Tel: 512-471-4929

Fax: 512-471-6548

e.rathje@mail.utexas.edu

<http://www.ce.utexas.edu/dept/area/geotech/GeotechnicalEngr.htm>

NEHRP Element: II

Key Words: Site Response, Random Vibration Theory, Probabilistic

Research supported by the U.S. Geological Survey (USGS), Department of the Interior, under USGS award number (04HQGR0071). The views and conclusions contained in this document are those of the authors and should not be interpreted as necessarily representing the official policies, either expressed or implied, of the U.S. Government

ABSTRACT

The objective of this research is to develop a site response computation module that can be coordinated with Open Seismic Hazard Analysis (OpenSHA). This site response module includes equivalent-linear site response calculations via traditional time domain procedures and newly developed random vibration theory (RVT) procedures. Additionally, the site response module includes the ability to incorporate frequency dependent soil properties (i.e., frequency dependent method (FDM), Kausel and Assimaki 2002), such that the nonlinear soil response can be better captured in an equivalent-linear procedure. RVT analysis is well-suited for PSHA because it predicts the site response without requiring any input time histories. FDM equivalent-linear analysis analysis also is well-suited for PSHA because it allows equivalent-linear analysis to be used for the larger input intensities modeled as part of PSHA.

The site response module was developed in Matlab and used to perform a series of site response calculations for validation. For validation, RVT site response analysis was compared with traditional analysis using time domain input motions. Here, the comparison was favorable, with some slight overprediction of site response by RVT at periods close to the site period. The FDM procedure was implemented and used to predict the surface response at the Treasure Island site in San Francisco, California. In comparison with traditional equivalent-linear procedure, the FDM procedure does not experience overdamping of high frequencies and provides more realistic surface time histories of acceleration.

NON-TECHNICAL SUMMARY

Soil conditions can significantly affect the level of ground shaking at a site. Site response procedures predict how the soil conditions (i.e., thickness, stiffness, layering, nonlinearity) impact the ground shaking at a site. Current probabilistic assessments of ground shaking from earthquakes do not include the impact of soil conditions, although the soil conditions can changed the shaking intensity by more than a factor of 10. This project developed a site response module that predicts the effect of soil conditions on ground shaking, such that this effect can be incorporated into future probabilistic seismic hazard assessments.

INTRODUCTION

Open Seismic Hazard Analysis (OpenSHA) is a web-enabled, open-source probabilistic seismic hazard analysis (PSHA) code that is being developed jointly by USGS and SCEC (www.opensha.org). One of the goals of the OpenSHA project is to develop a computational infrastructure that allows different SHA components to be plugged into an analysis, so that researchers can evaluate the sensitivity of hazard to alternative models of the various components in a PSHA. The current structure of the OpenSHA is focused on the geological and seismological models in a PSHA. To open the OpenSHA framework to geotechnical engineers, such that geotechnical engineers can evaluate the effect of geotechnical site characterization on PSHA results, a site-specific geotechnical site response module was developed.

The developed OpenSHA module for geotechnical site response was written in Matlab and propagates seismic waves through a one-dimensional soil profile using the equivalent-linear approach with nonlinear shear modulus reduction and damping curves. All analyses are performed in the frequency domain. The module incorporates a random vibration theory (RVT) site response procedure (Schneider et al. 1991, Silva et al. 1997), which is well-suited for PSHA because it does not require a suite of time-domain input ground motions. Rather, the RVT site response procedure uses a Fourier amplitude spectrum, one-dimensional wave propagation, and random vibration theory to develop stable estimates of site response. This RVT procedure was incorporated into the site response module and validated against results from site response analyses using time domain motions (Rathje and Ozbey 2006, Ozbey 2006).

Equivalent-linear site response analysis in the frequency domain suffers from overdamping of high frequency motions when large intensity input motions are used. Kausel and Assimaki (2002) indicate that equivalent-linear analysis with frequency-dependent material properties (i.e. called the frequency dependent method, FDM) can overcome this shortcoming and provide site response results that are similar to those from fully nonlinear analysis. Thus, FDM equivalent-linear analysis is well-suited for PSHA because it allows equivalent-linear analysis to be used for the larger input intensities modeled as part of PSHA. The FDM procedure was included in the module and site response comparisons from FDM were compared with traditional equivalent-linear analysis and strong motion recordings at a soil site from a previous earthquake.

RANDOM VIBRATION THEORY (RVT) SITE RESPONSE

Random Vibration Theory (RVT)-based site response is an extension of stochastic ground motion simulation procedures developed by seismologists to predict peak ground motion parameters as a function of earthquake magnitude and site-to-source distance (e.g. Hanks and McGuire 1981, Boore 1983). The RVT procedure consists of characterizing the Fourier Amplitude Spectrum (FAS) of a motion and using RVT to compute peak time domain values of ground motion from the FAS. When site response is included in the calculation, the FAS developed from source theory is modified to account for the soil response before RVT is applied.

Traditional site response analysis in geotechnical practice assumes one-dimensional wave propagation and computes the acceleration-time history and acceleration response spectrum at the surface of a soil deposit. In geotechnical practice, the most commonly used site response procedure involves one-dimensional transfer functions for a layered soil deposit (e.g. SHAKE91,

Idriss and Sun 1992). For this analysis, an outcropping rock acceleration-time history is specified to drive the analysis; therefore, it can be considered a time history site response analysis, although the computations are performed in the frequency domain. A schematic of this procedure is shown in Figure 1(a), where the rock acceleration-time history is specified, propagated through the soil to the ground surface, and the time history surface motion is used directly to compute the acceleration response spectrum at the ground surface. In this analysis, the nonlinear response of the soil is approximated by strain-compatible, equivalent-linear soil properties. Generally, a suite of scaled input motions is used that match, on average, the median rock response spectrum, or a smaller number of spectrally matched motions is used. The target response spectrum for the input motions may be a deterministic response spectrum from a ground-motion prediction equation or a uniform hazard spectrum from probabilistic seismic hazard analysis.

Random Vibration Theory represents an alternative approach to calculate site response. In the RVT approach, the input to the site response analysis is a single Fourier amplitude spectrum (FAS) that represents the input rock motion. This spectrum contains only the Fourier amplitudes, without the accompanying phase angles, and thus cannot be used to compute directly an acceleration-time history. However, RVT can be used to estimate peak time domain values from the Fourier amplitude information. A schematic of RVT-based site response analysis is shown in Figure 1(b). Transfer functions are used to propagate the FAS through the soil column to obtain the FAS of the motion at the ground surface, and RVT is utilized to calculate peak time domain parameters, such as peak ground acceleration and spectral acceleration, from the FAS. The product of an RVT-based site response analysis is an acceleration response spectrum calculated from the surface FAS, rather than an acceleration-time history.

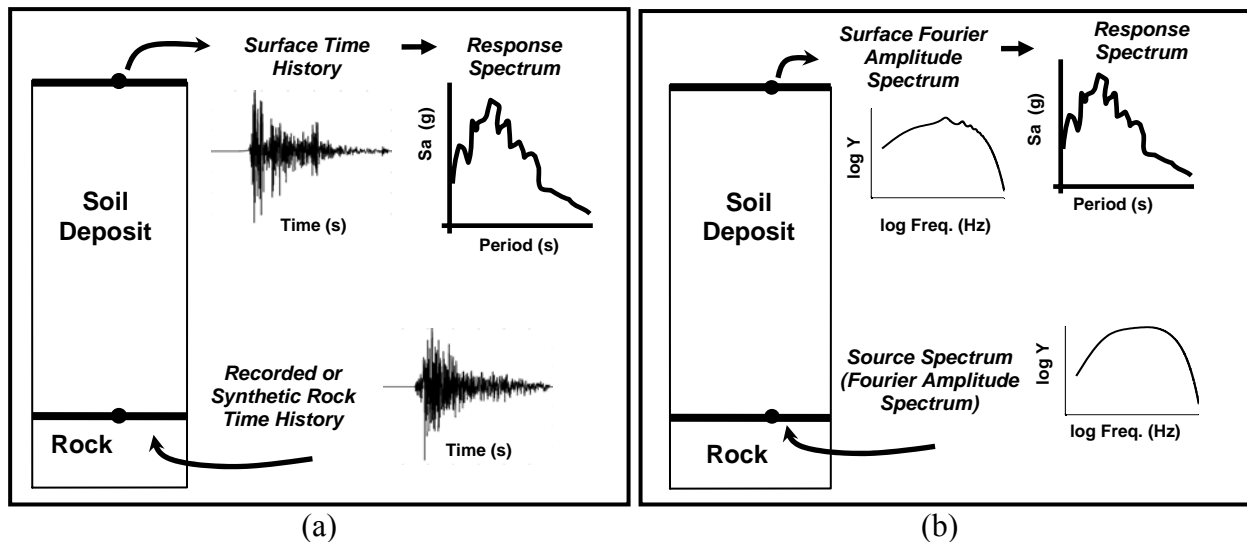


Figure 1. (a) Time History Seismic Site Response Analysis, and (b) Random Vibration Theory Based Seismic Site Response Analysis.

Principles of Random Vibration Theory

The key to RVT analysis is the prediction of peak time domain motions from only a Fourier Amplitude Spectrum representation of the motion using extreme value statistics. Extreme value statistics was first used in seismology by Hanks and McGuire (1981) to predict

peak acceleration from the *rms* (root-mean-square) acceleration, a_{rms} . Parseval's theorem is used to compute a_{rms} from the Fourier amplitude spectrum, $Y(f)$, and a peak factor is used to relate a_{rms} to the peak ground acceleration (PGA). Parseval's theorem states that the energy is conserved in both the time and the frequency domains, resulting in the following expression:

$$a_{rms} = \sqrt{m_0 / T_{rms}} \quad (1)$$

where m_0 is the zero moment of the square of the FAS, $|Y(f)|^2$, and T_{rms} is the duration of motion. For peak acceleration, T_{rms} is set equal to the ground motion duration, T_{gm} . In this work we define T_{gm} as the source duration ($T_{gm} = 1/f_c + 0.05 \cdot R$, where R is distance in km), although other definitions would be equally valid. The n th moment of the square of the FAS is defined as:

$$m_n = 2 \int_0^{\infty} (2\pi f)^n |Y(f)|^2 df \quad (2)$$

The peak factor, which relates the peak value to the *rms* value through a ratio (peak/rms), is used to obtain the peak acceleration from the computed value of a_{rms} . One of the first RVT methods was proposed by Cartwright and Longuet-Higgins (1956) and this method was applied to ground motion simulation by Boore (1983, 2003). Cartwright and Longuet-Higgins (1956) considered the probability distribution of the maxima of a train of ocean waves and developed expressions for the peak factor in terms of the characteristics of the wave train. The expected value of the peak factor is computed using:

$$\text{Peak Factor} = \frac{a_{max}}{a_{rms}} = \sqrt{2} \int_0^{\infty} \{1 - [1 - \xi \exp(-z^2)]^{N_e}\} dz \quad (3)$$

$$\xi = \frac{N_z}{N_e} \quad (4)$$

In these expressions, ξ is the bandwidth factor, N_z is the number of zero crossings in the wave train, and N_e is the number of extrema. For a narrow band signal, N_z is equal to N_e and, thus, ξ is equal to 1.0. For signals with motion spread over a range of frequencies (such as earthquake motions), N_z is smaller than N_e and, thus, ξ is less than 1.0. N_z and N_e are derived from the frequencies of zero crossings and extrema (f_z and f_e , respectively) and ground motion duration (T_{gm}) using:

$$N_z = 2f_z T_{gm} \quad , \quad N_e = 2f_e T_{gm} \quad (5)$$

T_{gm} is taken as the source duration, given by $1/f_c + 0.05 \cdot R$, where R is distance (km). The parameters f_z and f_e are computed from the moments of the FAS using:

$$f_z = \frac{1}{2\pi} (m_2 / m_0)^{1/2} \quad , \quad f_e = \frac{1}{2\pi} (m_4 / m_2)^{1/2} \quad (6)$$

Generally, the expected value of the peak factor takes on values between 1.5 and 3.5, depending on the number of extrema and the bandwidth (Rathje and Ozbey 2006).

Input Motion Characterization

There are different methods available to describe the input FAS for RVT site response analysis. The simplest approach involves the use of seismology theory to compute the radiated FAS from a point source in terms of various source, path, and site parameters (EPRI 1993). Other techniques involve deriving the FAS from an acceleration response spectrum using inverse random vibration (IRVT) techniques (e.g., Gasparini and Vanmarcke 1976, Rathje et al. 2005) and finite fault seismological simulations (e.g., Beresnev and Atkinson 1998). For this study, input FAS were derived using the seismological point source model and the IRVT procedure.

Seismological Source Theory

This section represents a brief introduction to the terminology in seismological source theory and earthquake motion characterization, based on the description given by Boore (2003). The FAS of acceleration, $Y(f)$, at a rock site can be described analytically as a function of the source, propagation path, and site characteristics (the site characteristics in this case represent the effect of the near-surface rock layers and not the effect of the overlying soil layers). The Brune (1970, 1971) omega-squared (ω^2) source spectrum is the most common and simplest representation of the radiated FAS from an earthquake. This source spectrum, $E(M_0, f)$, is coupled with the effects of the propagation path, $P(R, f)$, high frequency diminution, $D(f)$, and crustal amplification, $A(f)$, resulting in what is often called a Brune spectrum:

$$Y(f) = E(M_0, f) P(R, f) D(f) A(f) \quad (7)$$

$$Y(f) = \left[0.78 \frac{\pi}{\rho_0 \beta_0^3} M_0 \frac{f^2}{1 + (f/f_c)^2} \right] \left[Z(R) \cdot \exp\left(\frac{-\pi f R}{Q(f) \beta_0}\right) \right] \left[\exp(-\pi \kappa_0 f) \right] A(f) \quad (8)$$

where f is frequency (Hz), ρ_0 is the mass density of the crust (g/cm^3), β_0 is the shear wave velocity of the crust (km/s), R is the distance from the source (km), $Z(R)$ is the geometric attenuation, $Q(f)$ is the anelastic attenuation, κ_0 is the diminution parameter (seconds) and M_0 is the seismic moment (dyne-cm). Seismic moment is related to moment magnitude (M_w) by:

$$M_0 = 10^{1.5M_w + 16.05} \quad (9)$$

Finally, f_c in equation 8 is the corner frequency (Hz), which represents the frequency below which the FAS of acceleration decays. The corner frequency is defined as:

$$f_c = 4.9 * 10^6 \beta_0 (\Delta\sigma / M_0)^{1/3} \quad (10)$$

where $\Delta\sigma$ is the stress drop (bars). The expressions above assume a point source for the earthquake and include only a single corner frequency.

Typical values of the parameters required for equations 8 through 10 for Western North America (WNA) are given in Table 1 (Campbell 2003). The amplification function, $A(f)$, in equation 8 accounts for the propagation of waves from the deeper crust, where the shear wave

velocity of the rock is on the order of 3500 m/s, to the near surface, where the shear wave velocity of competent rock is generally 750 m/s. Suggested values of $A(f)$ for generic rock sites in WNA can be found in Boore and Joyner (1997). These amplification values generally range between 1.0 and 4.0 over the frequency range of engineering interest. Although some of the parameters in Table 1 represent the effect of path or site characteristics, for brevity they will be called source parameters.

Beyond earthquake magnitude and site-to-source distance, the most important parameters affecting the shape of the Brune spectrum are the stress drop ($\Delta\sigma$) and the diminution parameter (κ_0). The stress drop affects the corner frequency (equation 10), which in turn affects the moderate to high frequency portions of the spectrum (i.e., above about 0.3 Hz). The diminution parameter affects higher frequencies (i.e., above about 10 Hz) through its frequency dependent exponential form (equation 8).

Table 1. Baseline seismological source and path parameters used in this study

Parameter	Value
Density, ρ (g/cc)	2.8
Shear wave velocity, β_0 (km/s)	3.5
Stress drop, $\Delta\sigma$ (bar)	100
Diminution parameter, κ_0 (s)	0.04
Geometric attenuation, $Z(R)$	R^{-1} for $R < 40$ km $R^{-0.5}$ for $R \geq 40$ km
Anelastic attenuation, $Q(f)$	$180 * f^{0.45}$

Inverse Random Vibration Theory

Inverse RVT (IRVT) takes an acceleration response spectrum and converts it into a frequency domain FAS (Figure 2). While it is relatively straight forward to produce a response spectrum from a FAS, it is not trivial to perform the inverse. There are two complications for the inversion. First, the spectral acceleration is influenced by a range of frequencies in the FAS, such that a spectral acceleration at a given period cannot be related solely to the Fourier amplitude at the same period. To solve this problem, the IRVT procedure takes advantage of some of the properties of single-degree-of-freedom (SDOF) transfer functions (TF). Specifically, the SDOF transfer function is narrow band for lightly damped systems and it goes to zero at frequencies much larger than the natural frequency, which limits the frequency range that affects the spectral acceleration at a given period. The second complication is that the peak factor cannot be determined apriori because it is based on the FAS, which is unknown. However, a peak factor can be assumed to develop an initial estimate of the FAS and then this spectrum can be used in a second iteration to compute peak factors for use in the inversion. The IRVT methodology described below is based on the procedure proposed by Gasparini and Vanmarcke (1976) and described by Rathje et al. (2005).

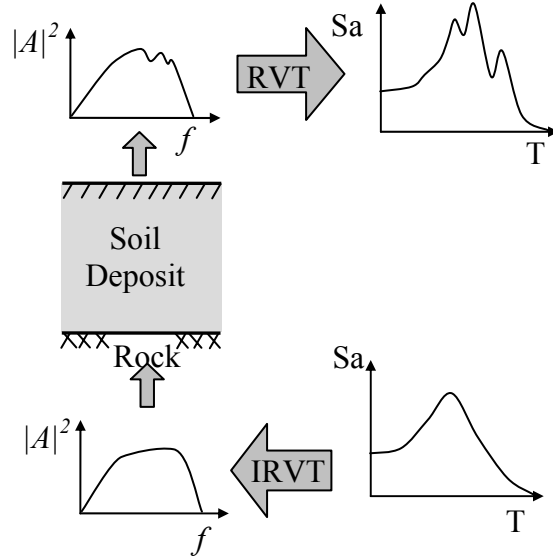


Figure 2. The application of IRVT to derive the input FAS for an RVT site response analysis.

Using the characteristics of SDOF transfer functions and an assumed, or known peak factor, the square of the Fourier amplitude at the SDOF natural frequency, $|A(f_n)|^2$, can be written in terms of the spectral acceleration (Sa) at f_n , the peak factor (pf), the duration of motion (T_d), the Fourier amplitudes, $|A(f)|^2$, at frequencies less than f_n , and the integral of the SDOF transfer function.

$$|A(f_n)|^2 \approx \frac{1}{\int_0^\infty |H_{fn}(f)|^2 df - f_n} \left(\frac{T_d}{2} \frac{Sa^2}{pf^2} - \int_0^{f_n} |A(f)|^2 df \right) \quad (11)$$

The transfer function integral is a constant for a given natural frequency and damping ratio, allowing the equation to be simplified to:

$$|A(f_n)|^2 \approx \frac{1}{f_n \left(\frac{\pi}{4\xi} - 1 \right)} \left(\frac{T_d}{2} \frac{Sa^2}{pf^2} - \int_0^{f_n} |A(f)|^2 df \right) \quad (12)$$

Equation (12) is applied first at low frequencies, where the integral term can be assumed equal to zero, and then at successively higher frequencies. In the calculations that were performed in this study the frequency range was composed of 500 points equally spaced in log space. The minimum and maximum frequencies corresponded to the minimum and maximum periods in the input response spectrum.

The computed FAS from IRVT produces a response spectrum that deviates 5 to 10% from the input target response spectrum. To improve the predicted response spectrum, a correction is applied to the FAS based on the error in the response spectrum. Although the spectral acceleration at a given frequency does not directly translate into the FAS at that frequency, the spectral ratio ($Sa_{input} / Sa_{predicted}$) was used to modify the FAS. Using this correction, when the predicted response spectrum is smaller than the input response spectrum,

the FAS is increased, and when the predicted response spectrum is greater than the input response spectrum, the FAS is reduced. By squaring the ratio, convergence is achieved more quickly (Gasparini and Vanmarcke 1976). The squared spectral ratio is defined as:

$$r = \left(\frac{Sa_{input}}{Sa_{predicted}} \right)^2 \quad (13)$$

where Sa_{input} is the input spectral acceleration at a given period and $Sa_{predicted}$ is the calculated spectral acceleration from the IRVT FAS at the same period. The FAS is corrected using:

$$|A(f)_{corr.}| = r \cdot |A(f)_{predicted}| \quad (14)$$

This process is repeated until the desired accuracy is achieved. In this study, the correction is applied until a maximum error of 2% is reached or 20 iterations are performed.

Input Motion Comparisons

To compare the two input motion characterizations, the two procedures were used to develop input FAS to match acceleration response spectra from the Abrahamson and Silva (1997) ground motion prediction equation for three magnitude and distance combinations (M_w 6.5 and R 5 km, M_w 6.5 and R 60 km, M_w 7.5 and R 60 km). For the seismological point source characterization, the input parameters in Table 1 were used, except that the stress drop ($\Delta\sigma$) and the diminution parameter (κ_0) were varied in order to get the best match with each target acceleration response spectrum.

The derived Fourier amplitude spectra from both techniques (Brune seismological spectra, IRVT spectra), along with their corresponding acceleration response spectra, are shown in Figure 3. The target Abrahamson and Silva (1997) spectrum is also shown, and for the Brune spectra the values of $\Delta\sigma$ and κ_0 that produce the best fit are listed. The RVT response spectra are in excellent agreement with the input response spectra from Abrahamson and Silva (1997), with the spectra being almost indistinguishable. For the seismological Brune spectrum characterization, even with the best-fit $\Delta\sigma$ and κ_0 parameters, the resulting response spectra deviate from the target response spectra. The most noticeable differences occur at low and high frequencies.

In comparing the FAS from IRVT and the Brune point source model at smaller magnitudes (M_w 6.5, Figs. 3a and b), the spectra match at lower frequencies but start to diverge at larger frequencies. The corner frequency and stress drop control the low frequency part of the spectrum, and thus this favorable comparison indicates that the form of the Brune spectrum in terms of these parameters is adequate for this magnitude. The diminution parameter, along with $Q(f)$, control the large frequency part of the spectrum. The deviation of the Brune and IRVT spectra in this frequency range appears to indicate that the $\exp(-\pi\kappa_0 f)$ form of equation (8) is inadequate. As some seismologists consider this term simply a fitting term, and other forms of this term have been used in the past (Boore 1983), perhaps it is not surprising that this term is somewhat inadequate. For the larger magnitude event (M_w 7.5, Figure 3c), the Brune spectrum is significantly larger than IRVT at lower frequencies, which results in significantly larger spectral accelerations at low frequencies (Figure 3f). The overprediction of the FAS at low frequencies for larger magnitude earthquakes occurs because of the breakdown of the point source

assumption (Boore 1983). To address this issue, a two corner frequency model has been proposed (Atkinson and Silva 1997). Thus, it appears that the FAS developed from ground motion prediction equations at large magnitudes are in agreement with the two corner frequency model.

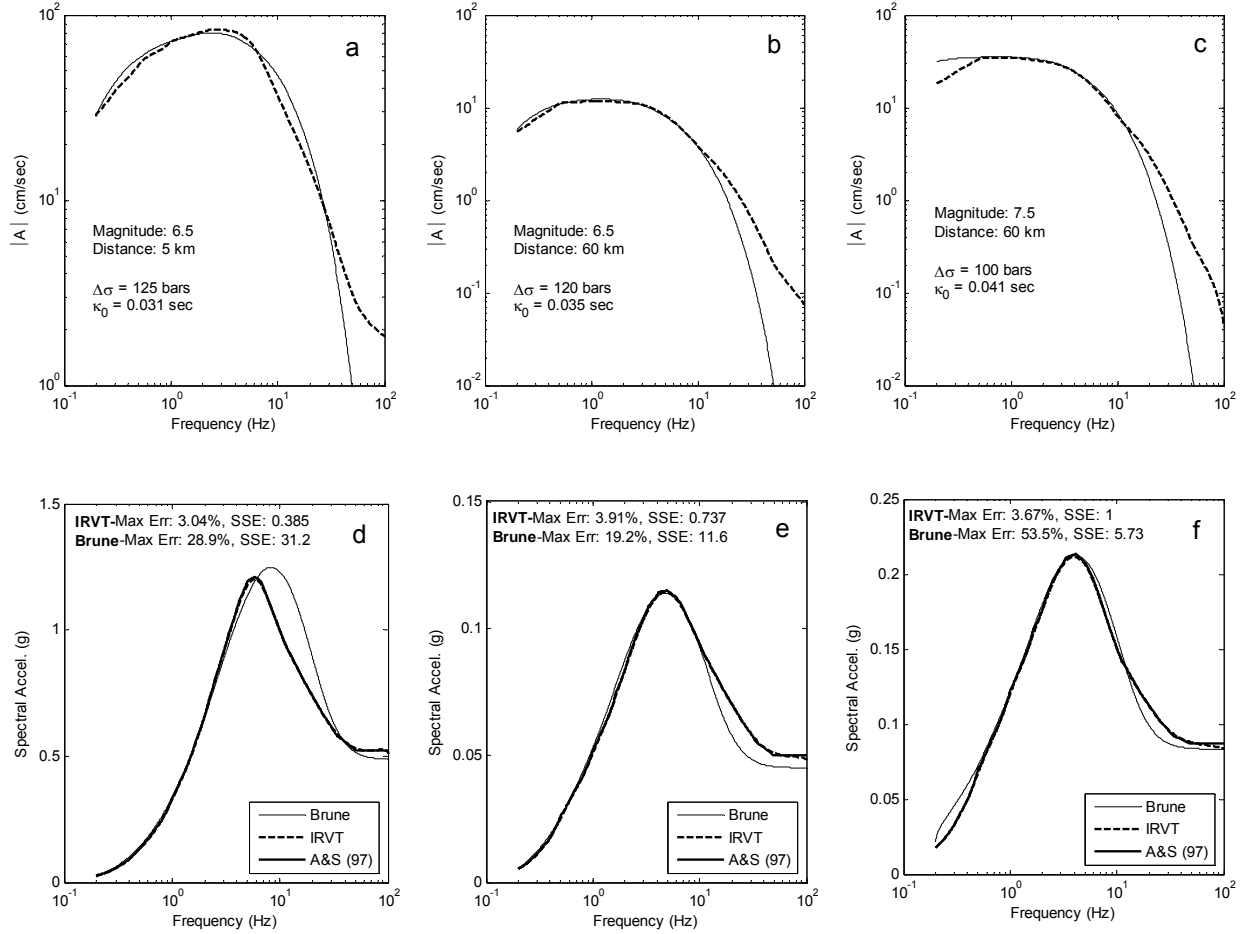


Figure 3. Comparison of Fourier amplitude spectra and acceleration response spectra from the seismological point source model and IRVT.

Site Response Predictions

Random vibration theory applied to site response analysis predicts the response spectrum at the top of the soil deposit. In conventional time history site response analysis, an acceleration-time history is prescribed at the base rock, propagated to the ground surface to compute an acceleration-time history at the surface, and this time history is used to compute an acceleration response spectrum. The propagation of the motion to the ground surface can be performed using the equivalent linear approach implemented in the frequency domain or the fully nonlinear approach implemented in the time domain. Because RVT-based site response analysis can only be performed in the frequency domain, it is limited to equivalent-linear site response analysis and cannot be used with fully nonlinear analysis.

The acceleration response spectrum at the ground surface in RVT-based site response analysis is computed from the square of the FAS of motion at the ground surface (i.e., $|Y_{surf}(f)|^2$).

This surface FAS is calculated from the FAS at the base rock and the amplitude of the transfer functions (i.e. $|F_{ij}(f)|^2$, where i and j are soil layers) that represent 1D wave propagation through the soil deposit. The transfer functions are similar to those used in traditional site response programs such as SHAKE91 (Idriss and Sun 1992), and the input FAS is prescribed as an outcrop motion. The major difference between using a time history input motion and using an FAS input motion is the phase information. For conventional analysis with time history input motions, the phase information for the FAS is known and the transfer function transfers both amplitude and phase information to the surface. When only amplitude information is known, which is the case for the FAS used in RVT analysis, only the amplitude information is propagated to the surface by the transfer functions.

In any equivalent-linear site response analysis, the shear strains in each layer must be computed to select equivalent-linear soil properties that account for soil nonlinearity. In RVT-based analysis, these strains are computed using transfer functions that compute the shear strain in each layer. The result is a FAS for shear strain for each layer and RVT is used to calculate the peak time domain shear strain from the *rms* shear strain. Similar to traditional equivalent-linear procedures, the peak shear strain is reduced to an effective shear strain to choose strain compatible soil properties. Iterations are performed until the equivalent-linear soil properties are compatible with the shear strains generated in the soil. For this study, a program was developed in MATLAB that computes equivalent-linear RVT and time domain site response.

The Treasure Island soft soil site was analyzed to compare RVT and traditional time history seismic site response analysis. Treasure Island is a strong motion site located in the middle of San Francisco Bay, California. The soil properties and soil profile given by Dickenson (1994) were used to define the Treasure Island site. The schematic soil profile (Dickenson 1994) is given in Figure 4. The average shear wave velocity of the top 30 m is calculated as 160 m/s, which classifies the site as Site Class E (soft soil) in the IBC (2003) site classification system. The soil profile is approximately 100 m deep and was divided into 46 layers. The modulus reduction and damping curves used for the Treasure Island site are tabulated in Table 2 and shown in Figure 5. These curves were used by Dickenson (1994) to obtain a good match with recordings at Treasure Island during the 1989 Loma Prieta earthquakes; thus, these curves were used in this study.

Two earthquake scenarios were considered for the comparison of RVT-based and traditional equivalent-linear site response analyses. The first scenario, $M_w = 6.5$ and $R = 5$ km, represents a moderate size earthquake at close distance with a peak ground acceleration in excess of 0.5 g. The target response spectrum for this scenario from the Abrahamson and Silva (1997) ground motion prediction equation, along with the response spectra from the selected time histories, IRVT, and a Brune spectrum ($\Delta\sigma = 125$ bars, and $\kappa_0 = 0.031$ s), are shown in Figure 6. The time histories are listed in Table 3. In addition to these input motions, three of the time histories were spectrally matched to the target response spectrum, noted in Table 3, and a suite of time histories were generated using the seismological program SMSIM (Boore 2002) that simulates motions based on a Brune point source spectrum. The second scenario, $M_w = 7.5$ and $R = 50$ km, represents a large earthquake at further distance with a lower input intensity. The target response spectrum for this scenario from the Abrahamson and Silva (1997) ground motion prediction equation, along with the response spectra from the selected time histories IRVT, and a Brune spectrum ($\Delta\sigma = 100$ bars, and $\kappa_0 = 0.045$ s), are shown in Figure 7. The time histories are listed in Table 4 and the three spectrally matched motions are noted in this table. SMSIM motions were also generated for this scenario.

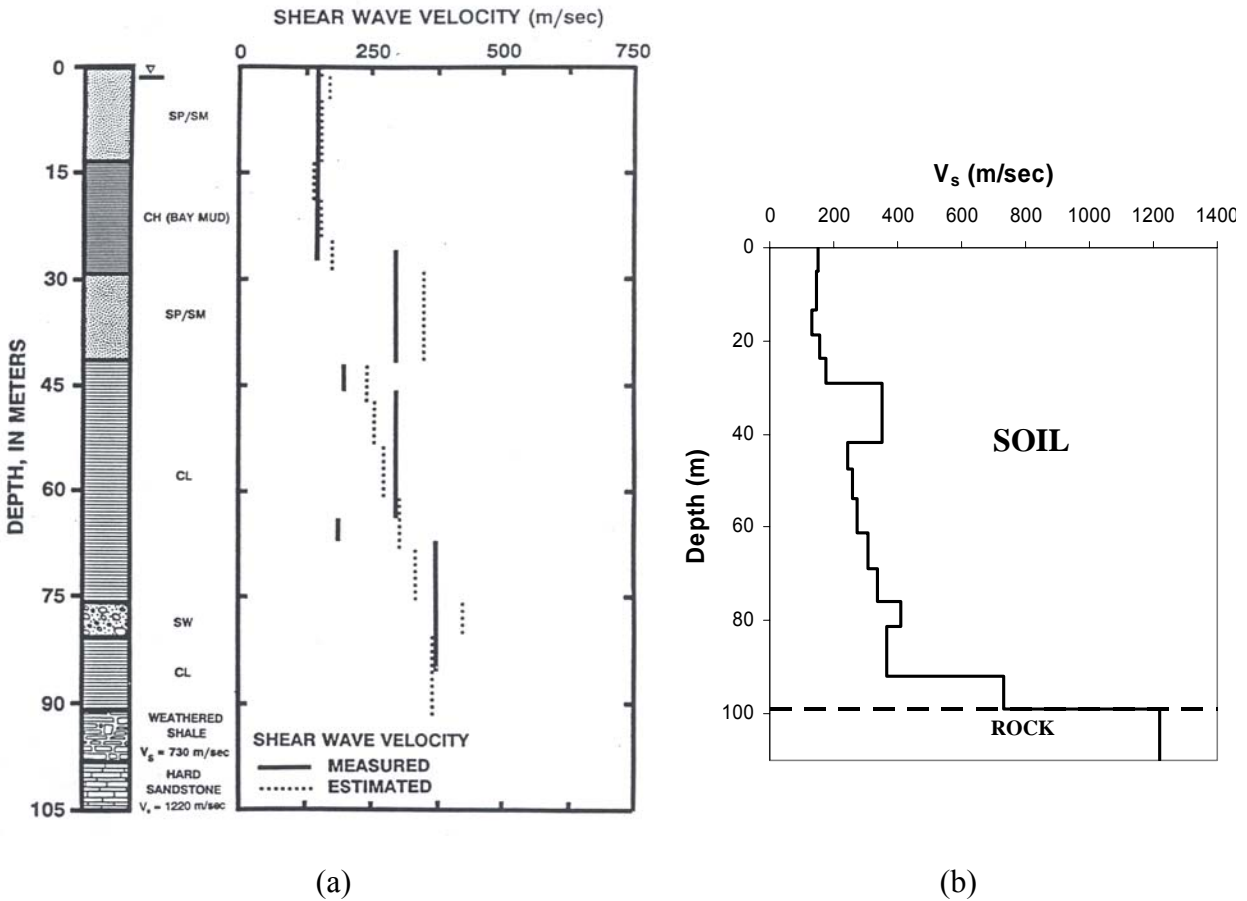


Figure 4. (a) Schematic soil profile and shear wave velocity profile at the Treasure Island Site (Dickenson 1994), (b) Generalized shear wave velocity profile used in analysis

Table 2. Modulus reduction and damping curves for the Treasure Island site (Dickenson 1994)

Material	Modulus Reduction	Damping
Sand (0-5 m)	Sand, $\sigma' < 1$ ksc (Seed et al. 1984)	Sand, Average (Seed & Idriss 1970)
Sand (5-13 m)	Sand, $1 < \sigma' < 3$ ksc (Seed et al. 1984)	Sand, Average (Seed & Idriss 1970)
Bay Mud (13-29 m)	Young Bay Mud (Sun et al. 1988)	Young Bay Mud (Sun et al, 1988)
Sand (29-42 m, 76-81 m)	Sand, $\sigma' > 3$ ksc (Seed et al. 1984)	Sand, Average (Seed & Idriss 1970)
Clay (42-76 m, 81-92 m)	Clay PI =20-40 (Sun et al. 1988)	Clay, PI=30, OCR=1-8 (Vucetic & Dobry 1991)
Rock	Rock (Schnabel 1973)	Rock (Schnabel 1973)

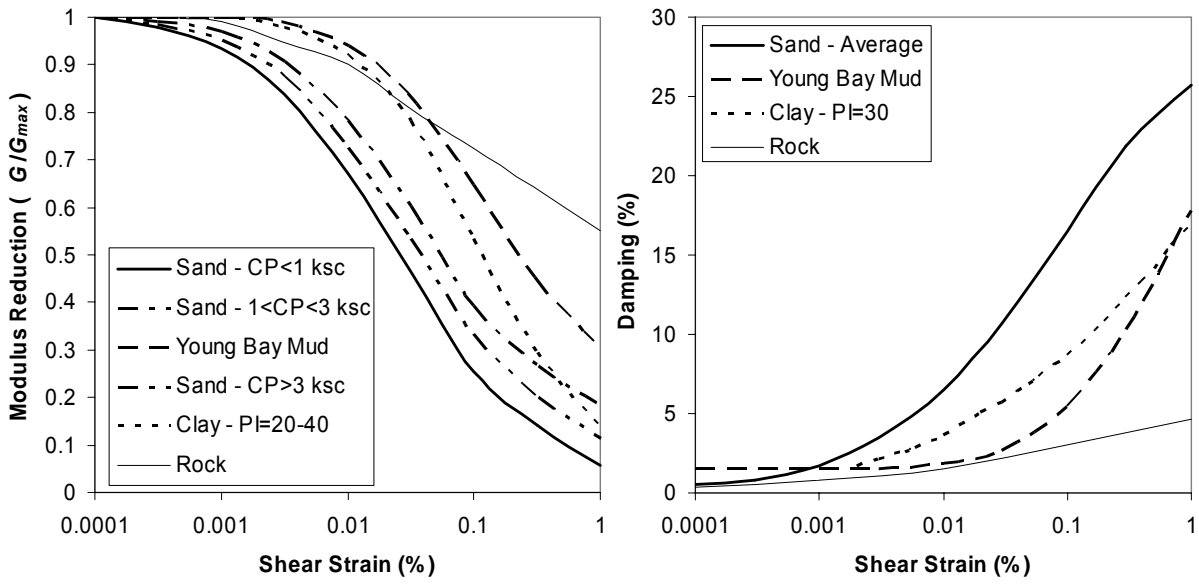


Figure 5. (a) Modulus reduction and (b) damping curves used in this study

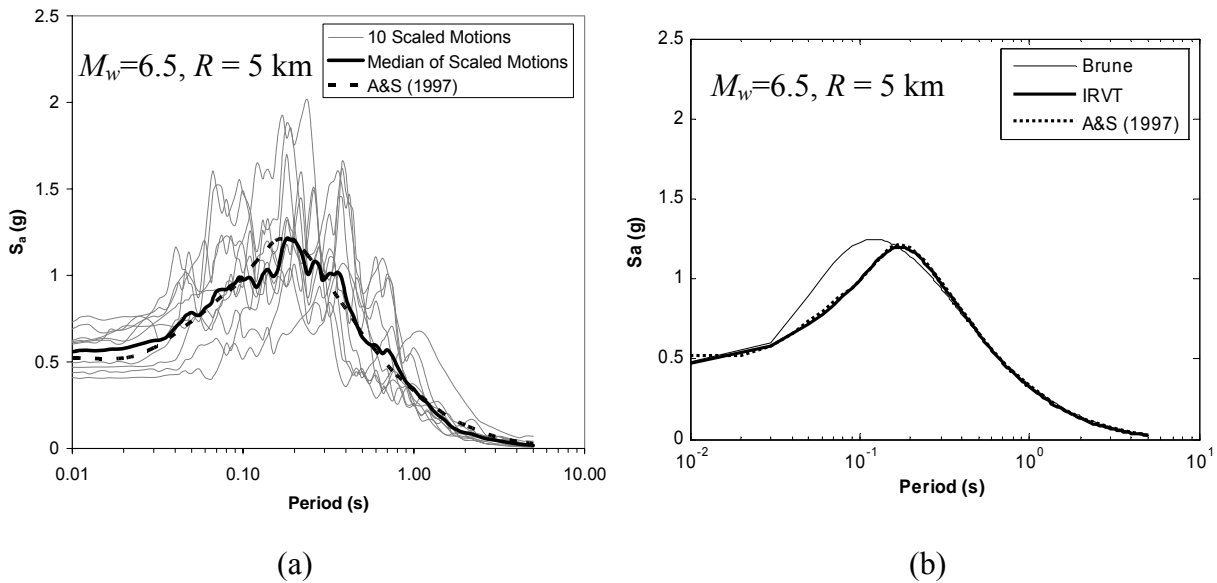


Figure 6. $M_w = 6.5$ and $R = 5$ km scenario input rock acceleration response spectra (a) scaled time history motions, (b) IRVT and Brune input spectra

Table 3. Scaled motions used for the $M_w = 6.5$ and $R = 5$ km scenario

Station, Component	Earthquake	M_w	R (km)	Geomatrix Site Class
Gilroy Array #6, 000 *	1984 Morgan Hill	6.2	11.8	B
Simi Valley-Kather. Rd, 000	1994 Northridge	6.7	14.6	B
Tarzana, Cedar Hill, 360	1994 Northridge	6.7	17.5	B
Pacoima Dam, 164	1971 San Fernando	6.6	2.8	B
Site 1, 010	1985 Nahanni, Canada	6.8	6.0	A
Site 1, 280	1985 Nahanni, Canada	6.8	6.0	A
Pasadena-Old Sei. Lab, 270	1971 San Fernando	6.6	19.1	A
Pacoima Dam (dwnstr) 265*	1994 Northridge	6.7	8.0	A
Superstition Mtn., 045	1987 Superstition Hills	6.7	4.3	A
Superstition Mtn., 135*	1987 Superstition Hills	6.7	4.3	A

* Motions used for spectral matching

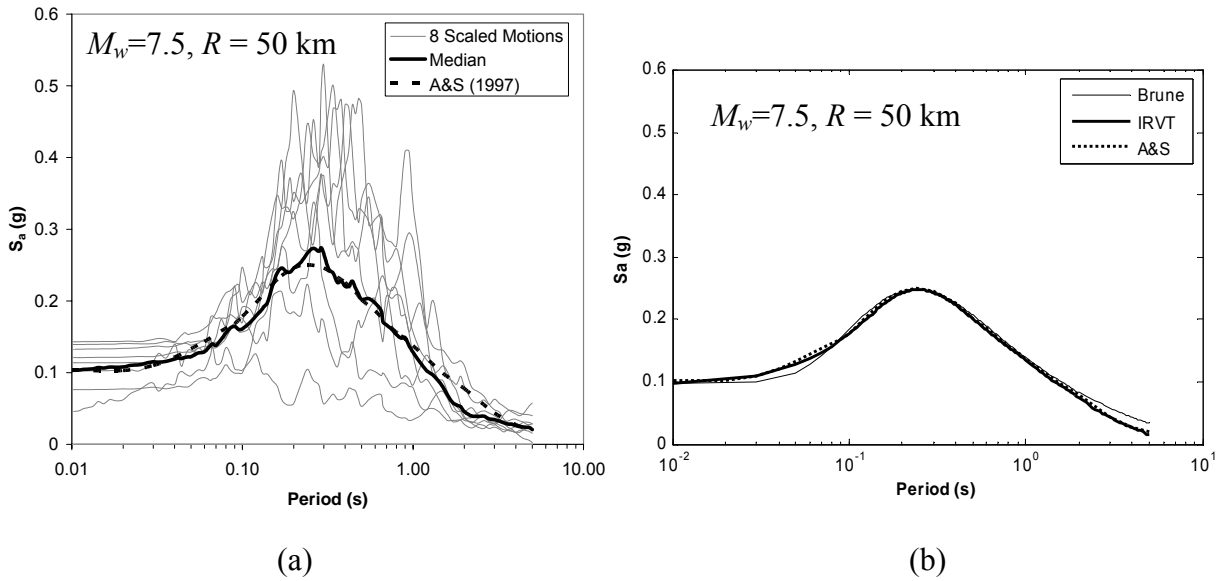


Figure 7. $M_w = 7.5$ and $R = 50$ km scenario input rock acceleration response spectra (a) scaled time history motions, (b) IRVT and Brune input spectra

Table 4. Scaled motions used for the $M_w = 7.5$ and $R = 50$ km scenario

Station, Component	Earthquake	M_w	R (km)	Geomatrix Site Class
Lamont Station 1060, N	1999 Duzce	7.1	30.2	A
CWB HWA026, N*	1999 Chi-Chi	7.6	58.8	A
CWB HWA046, E	1999 Chi-Chi	7.6	59.0	A
CWB HWA046, N	1999 Chi-Chi	7.6	59.0	A
CWB TCU025, N	1999 Chi-Chi	7.6	54.0	A
CWB TCU025, W*	1999 Chi-Chi	7.6	54.0	A
CWB TTN041, N	1999 Chi-Chi	7.6	54.0	A
Mecidiyekoy, 090*	1999 Kocaeli	7.4	62.3	B

* Motions used for spectral matching

The RVT-based surface acceleration response spectra and the median response spectra from the time history analyses for the $M_w=6.5$ and $R=5$ km earthquake scenario are shown in Figure 8. The surface response spectrum for RVT-based site response analysis using an input Brune spectrum and the median response spectrum from the SMSIM motions are shown in Figure 8(a). The results from these two analyses are shown separately because both use the same Brune (1970, 1971) seismological spectrum to characterize the input rock FAS. The response spectra in Figure 8(a) are in excellent agreement with some slight disagreement between periods of 0.7 and 1.5 s. The response spectra for the analyses that used scaled motions, spectrally matched motions, and IRVT (i.e., response-spectrum-compatible-input) are shown in Figure 8(b). The analyses with response-spectrum-compatible-input showed more variability (Figure 8(b)). The largest discrepancy is observed for the scaled input motions at periods greater than 0.25 s. The response from the scaled input motions displays two peaks at $T\sim 0.4$ s and $T\sim 0.75$ s and appears to be missing a peak at $T\sim 1.7$ s. These differences appear to be due to minor deviations of the scaled input motions from the prescribed target rock spectrum (Figure 6) and highlight the importance of input motion selection on the computed response.

Because of variations in the input rock response spectra for the various analyses, amplification factors were computed. Amplification factors are defined as the ratio of the surface spectral acceleration to the input rock spectral acceleration at each period and are shown in Figure 9 for this scenario. These results are more similar than the spectral accelerations (Figure 8) across the different input motion characterizations. The amplification factors for all five suites of analyses are in excellent agreement for periods less than the site period, but differ noticeably around the site period ($T\sim 1.8$ s). In this period range, the amplification factor for the RVT analysis with Brune input is 4.1, while the value is much smaller (Amp = 3.45) for the SMSIM input motions (Figure 9(a)). For the RVT analysis with IRVT input, the amplification at the site period is about 4.15, which is similar to the value for the spectrally matched input motions (Amp = 4.0) but is much larger than from the scaled input motions (Amp = 3.58). The amplification from RVT is about 15 to 20% larger than those from the scaled and SMSIM input motions, but only about 3% larger than the spectrally matched motions.

To consider the uncertainty in the median amplification factors, the 95% confidence intervals of the median amplification factors at the site period for the SMSIM and scaled input motions are also shown in Figure 9. The confidence interval represents the interval of possible

values for the median amplification factor with a confidence level of 95%. The confidence intervals are based on a t -distribution (Devore 1995), assuming the amplification factors for the SMSIM and scaled input motions follow a lognormal distribution. A lognormal distribution was assumed as the peak accelerations of earthquake ground motions are assumed to follow a lognormal distribution (Abrahamson 1987). The standard deviation (σ) used in the confidence interval calculation is the standard deviation of the natural logarithm of the amplification factors at the site period divided by the square root of the number of motions. The upper limits of the 95% confidence intervals for both the SMSIM and scaled input motions are smaller than the RVT predictions, indicating the differences between the time domain and RVT analyses are statistically significant.

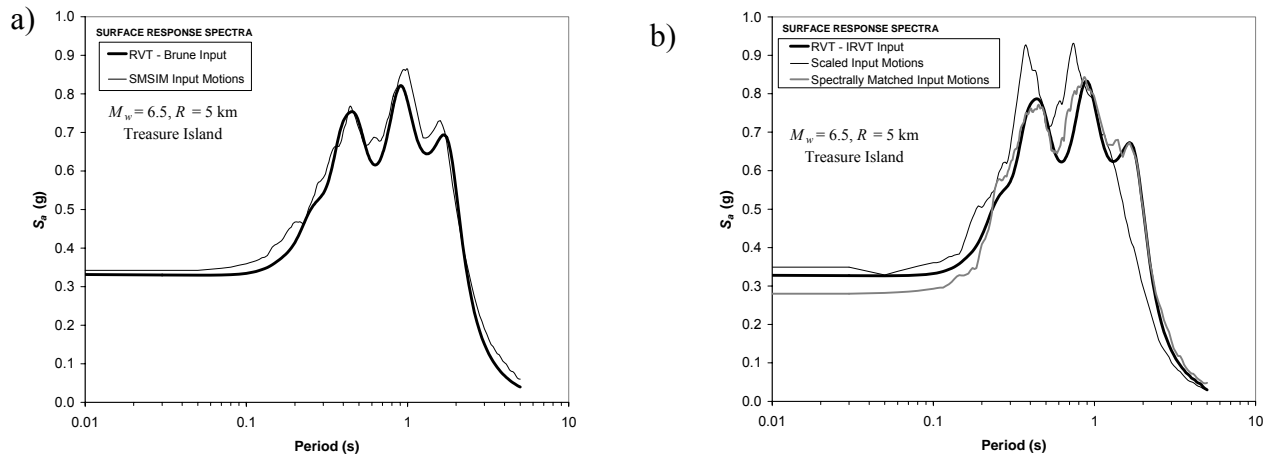


Figure 8. Median surface response spectra for RVT and time history analyses at the Treasure Island site ($M_w = 6.5, R = 5$ km)

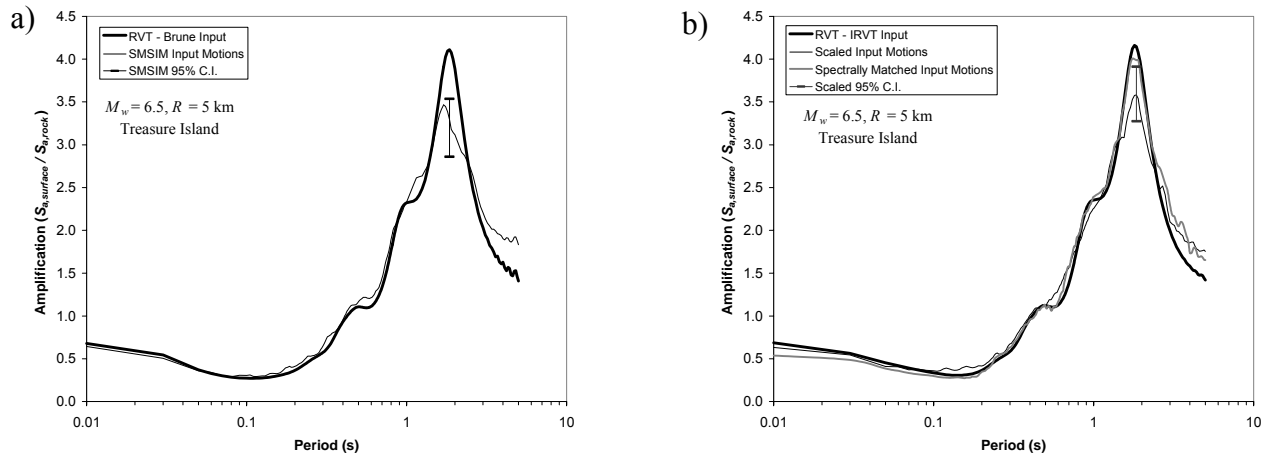


Figure 9. Amplification factors for RVT and time history analyses at the Treasure Island site ($M_w = 6.5, R = 5$ km)

Considering the induced shear strains, the median peak strains (averaged over each suite of time histories) are plotted versus depth in Figure 10. The strains that most influence the response of this site are the large strains in the soft soils near the surface. The largest strains occur at a depth of 12.5 m, where the soil is the softest (Figure 4). Here the SMSIM strains are the largest, the strains from the scaled motions are slightly smaller, and the strains from the spectrally matched input motions are about 20% lower. These strains correspond with the relative values of peak amplification in Figure 9; the SMSIM motions display the smallest amplification while the spectrally matched motions display the largest. The RVT strains at a depth of 12.5 m fall within the values from the time history analyses, although the RVT amplification is the largest.

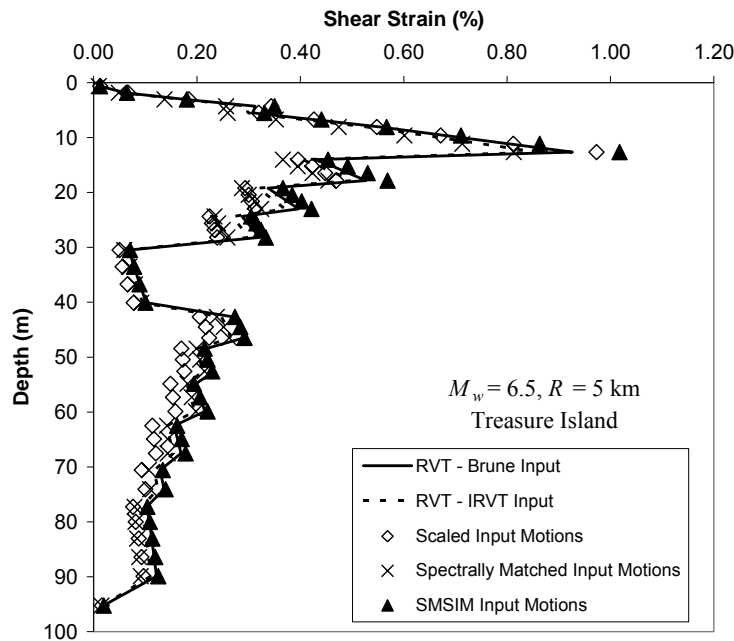


Figure 10. Shear strain from RVT and time history analyses at the Treasure Island site ($M_w = 6.5$, $R = 5$ km)

The RVT and median time domain response spectra for the $M_w=7.5$ and $R=50$ km earthquake scenario are shown in Figure 11. For both the Brune-input analyses (Figure 11(a)) and response-spectrum-compatible analyses (Figure 11 (b)), the surface response spectra agree favorably over most periods, except for the fundamental site period ($T \sim 1.5$ s). Here the site period is smaller than for the other scenario because of the lower intensity input motion, which induces less nonlinearity. At the site period, the scaled input motions exhibited the smallest values of spectral acceleration because these input motions were somewhat deficient in this period range (Figure 7). The amplification factors are shown in Figure 12. As for the other scenario, the amplification factors agreed well over all the periods except for the site period. For the Brune-input analyses, RVT again predicts amplification at the site period (Amp = 4.6) larger than the SMSIM time domain analyses (Amp = 4.19). For the analyses with response-spectrum-compatible input, the RVT results are largest at the site period (Amp = 4.7 for RVT, while Amp = 4.3 and 4.08 for spectrally matched and scaled input motions, respectively) and fall outside the

95% confidence interval from the time domain analyses. The amplification from RVT is about 10 to 15% larger than that predicted by the time domain analyses.

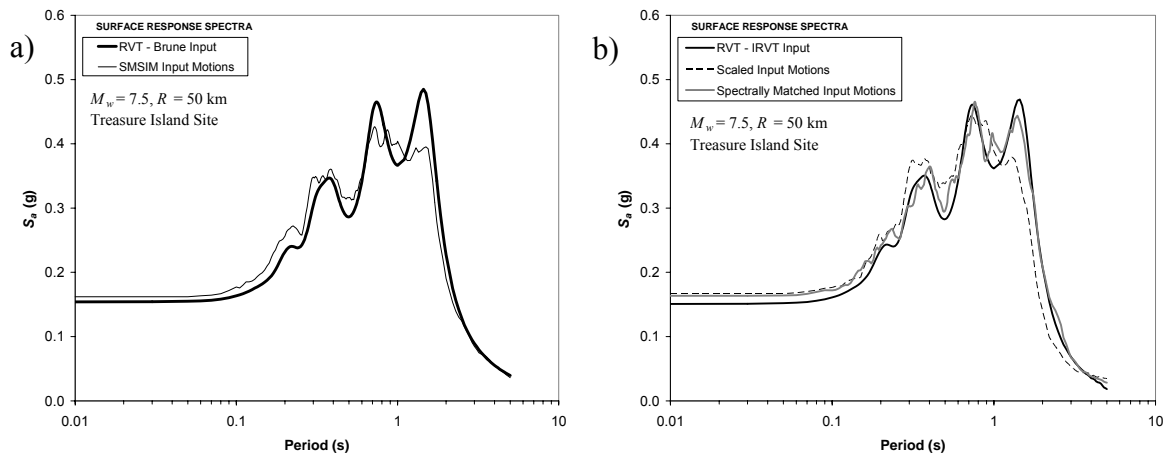


Figure 11. Median surface response spectra for RVT and time history analyses at the Treasure Island site ($M_w = 7.5$, $R = 50$ km)

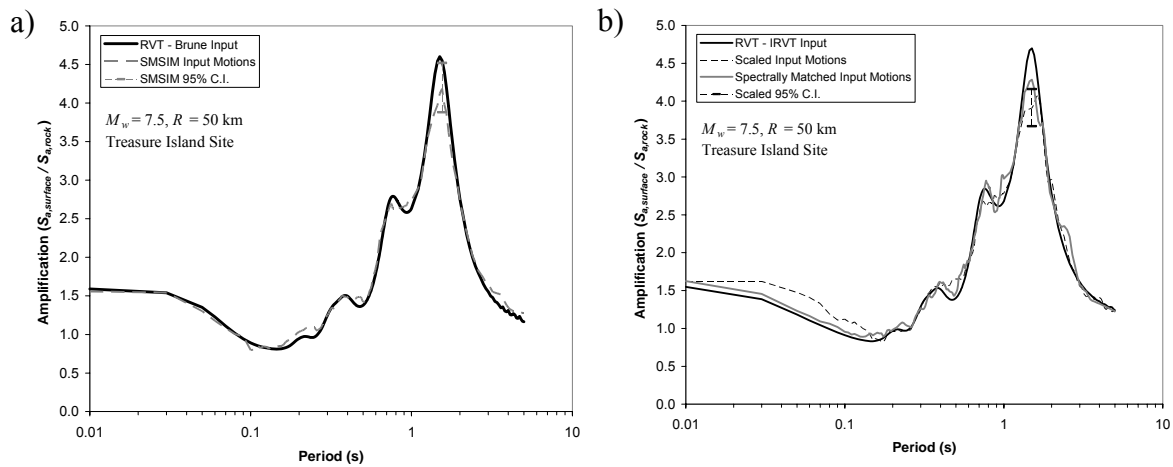


Figure 12. Amplification factors for RVT and time history analyses at the Treasure Island site ($M_w = 7.5$, $R = 50$ km)

The results from analyzing Treasure Island for two different earthquake scenarios that represent different levels of input intensity indicate that the amplification predicted by RVT is similar to the amplification produced by time domain analyses, except at periods close to the site period. In this period range, the RVT results indicate a bias that ranges from 5% to 30%. Further studies are required to assess the cause of this bias and to determine if it is significant.

FREQUENCY DEPENDENT METHOD (FDM) FOR SITE RESPONSE ANALYSIS

Site response analysis has been an integral part of seismic design studies since the 1970's. The development of the equivalent-linear (EQL) site response program SHAKE in 1972 initiated the wide spread use of site response analysis to evaluate the effect of soil conditions on strong ground motion. The SHAKE program is based on one-dimensional, linear elastic wave

propagation through layered media, but incorporates soil nonlinearity through the use of strain-compatible soil properties (i.e., shear modulus, G , and damping ratio, D). These soil properties are modified to be consistent with the shear strains generated by the earthquake shaking, and thus the strain-compatible properties model the shear modulus reduction and increased damping expected during strong shaking. The variations of shear modulus and damping ratio with shear strain are prescribed through modulus reduction and damping curves (Figure 13), and the shear strain used to select G and D is taken as a fraction of the peak time-domain shear strain. This strain is called the effective shear strain (γ_{eff}). Based on the strain-compatible soil properties for each layer, frequency domain transfer functions $[F_{ij}(\omega)]$ are used to model site response. These transfer functions prescribe the change in motion amplitude between layers i and j for each frequency, ω , and are used with the Fourier amplitude spectrum of the input motion to compute the motion at the ground surface.

SHAKE has been modified and improved over the years (e.g., SHAKE91, Idriss and Sun 1992; ProSHAKE, EduPro 1998), but the main computational scheme has remained the same. More sophisticated analytical techniques have been developed, such as fully nonlinear site response analysis (e.g., DESRA-2C, Lee and Finn 1991; SUMDES, Li et al. 1992; D-MOD, Matasovic and Vucetic 1995), but SHAKE-type equivalent-linear analysis remains the most common analytical procedure used to evaluate the effect of soil conditions on ground shaking and to develop site-specific, design-basis acceleration response spectra. However, there are significant concerns when using equivalent-linear analysis to compute site response for large magnitude earthquakes. Specifically, there are questions regarding the accuracy of EQL analysis at significant levels of shaking, which requires a modification to traditional EQL analysis.

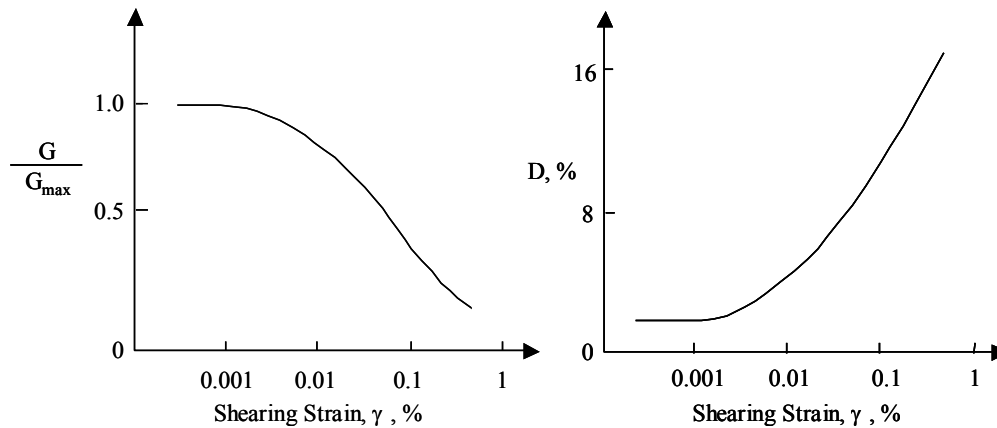


Figure 13. Typical modulus reduction and damping curves for soil

Although EQL site response analysis is widely used, it is truly accurate only at low to moderate levels of earthquake shaking. Equivalent-linear analysis does not provide an accurate estimate of site response at larger levels of shaking because, although nonlinearity is taken into account, the analysis remains, at its heart, a linear elastic analysis. The main difficulty arises from the selection of the strain-compatible soil properties used in the linear elastic analysis. As previously noted, these properties are selected based on the effective shear strain (γ_{eff}), which is defined as a fraction of the peak time-domain shear strain (γ_{max}). However, if one considers the frequency content of a typical shear strain-time history, it is readily apparent that shear strain amplitude varies significantly with frequency (Figure 14). The largest amplitudes tend to occur at lower frequencies, with the higher frequencies exhibiting shear strain amplitudes several

orders of magnitude smaller. The peak time-domain shear strain is most closely related to the frequencies with the largest amplitudes. Therefore, γ_{\max} and γ_{eff} represent the strains at low to moderate frequencies. However, this strain level is not appropriate for higher frequencies, which are strained significantly less (Figure 14). Nevertheless, the soil properties are chosen based on one value of γ_{eff} and these properties are applied to all frequencies. These properties are overly soft for the high frequency components of motion, and lead to overdamping of these high frequencies. The result is an underprediction of PGA and high frequency spectral acceleration. This difficulty with overdamping is mainly a concern at higher levels of shaking (i.e., $\text{PGA}_{\text{input}} \sim 0.4 \text{ g}$ and greater), where significant strains are generated. Therefore, fully nonlinear time domain analysis typically is performed to evaluate site response at higher levels of shaking.

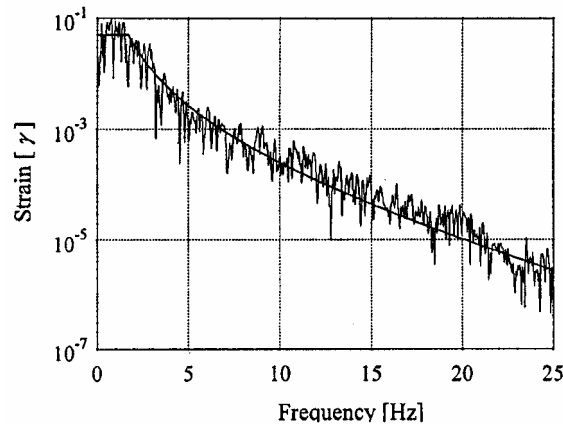


Figure 14. Fourier amplitude spectrum of shear strain-time history from 1994 Kobe N-S motion (from Kausel and Assimaki 2002)

Kausel and Assimaki (2002) describe a procedure to address this overdamping issue, called the frequency-dependent method (FDM). The FDM preserves the frequency domain EQL approach, but improves its accuracy at large strain levels. The FDM procedure prescribes frequency-dependent values of G and D based on the shear strain amplitudes generated at each frequency (e.g., Figure 14). These frequency-dependent material properties are not used to model any real frequency dependent material behavior, but to overcome the deficiencies of an EQL analysis. To consider the effect of incorporating frequency-dependent soil properties into EQL analysis, Kausel and Assimaki (2002) computed the response of a 1000-m deep soil site subjected to the Kobe N-S motion scaled to a PGA of 0.5 g. The response was computed using fully nonlinear analysis, EQL analysis with frequency-dependent material properties, and traditional EQL analysis with frequency-independent material properties. The computed surface acceleration-time histories are shown in Figure 15. The truly nonlinear and frequency-dependent models are almost indistinguishable (Figure 15(a)), indicating that frequency-dependent, EQL analysis can provide results consistent with fully nonlinear analysis, even for large intensity motions. The surface acceleration from the traditional EQL analysis is shown in Figure 15(b) and displays distinctly different characteristics. Due to overdamping of high frequencies, the PGA in Figure 15(b) is much smaller than the PGA from the other analyses, and the response shows almost no high frequency components of motion.

The Kausel and Assimaki (2002) study demonstrates the shortcomings of traditional EQL site response analysis and provides a powerful, yet simple, modification to overcome these shortcomings. The proposed modification of using frequency-dependent soil properties in EQL analysis (the FDM procedure) closely mimics the results from fully nonlinear analysis. As a result, frequency domain transfer functions, which are computationally efficient, can still be used to accurately model site response for the high intensities expected during large magnitude earthquakes.

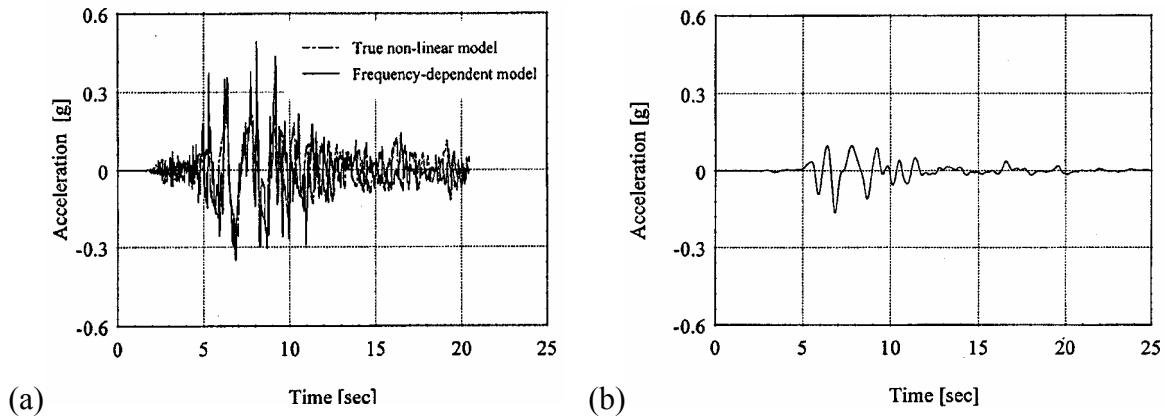


Figure 15. (a) Surface acceleration from true nonlinear and FDM-EQL analysis, (b) surface acceleration from traditional EQL analysis using frequency-independent properties (from Kausel and Assimaki 2002)

Site Response Comparisons

Although the FDM appears promising, the procedure has not been validated against strong motions recorded at soil sites during earthquakes. Towards this end, an analysis of the Treasure Island (TI) strong motion station in San Francisco was performed for the Loma Prieta earthquake, using the Yerba Buena Island (YBI) recorded as the input motion. The best-estimate shear wave velocity profile and nonlinear soil properties for the Treasure Island site are given in Figures 4 and 5, and in Table 2. This characterization of the site was assessed by Dickenson (1994) to provide the best match possible with the recorded motions from the Loma Prieta earthquake.

The input response spectrum from YBI000 and the surface recording from TI000 are shown in Figure 16, along with the predictions from traditional EQL and FDM EQL analyses. Note that in general both analyses underpredict the surface response with respect to the recorded motion; however, this difference may be a result in the YBI motion not accurately representing the underlying rock motion at TI. Nonetheless, the peak spectral acceleration from traditional EQL is close to the recorded spectral acceleration at the same period, but the lower period (higher frequency peaks) are significantly smaller than recorded. The FDM EQL results are similar to the traditional EQL results at long periods, but display larger values of spectral acceleration at lower periods. The spectral accelerations at $T = 0.3$ and 0.18 s are significantly larger, and the PGA is increased by about 15%.

The shear strain spectrum used to define the frequency-dependent material properties for the layer with the maximum strain is shown in Figure 17. For comparison, the effective strain used at all frequencies in the traditional EQL analysis is also shown. It is clear that the shear strains quickly decrease with increasing frequency, such that most of the strains are less than 10^{-4}

% at frequencies above 15 Hz. The smooth strain spectrum, which is fit to the Fourier amplitude of strain and employed to define the strains used to select the material properties, is also shown in Figure 17. The damping levels used at each frequency in the FDM analysis are shown in Figure 18(a) and the resulting surface to bedrock transfer functions for FDM and traditional EQL analysis are shown in Figure 18(b). In traditional EQL analysis, the damping is set equal to about 10% at all frequencies based on the effective shear strain. Because of this level of

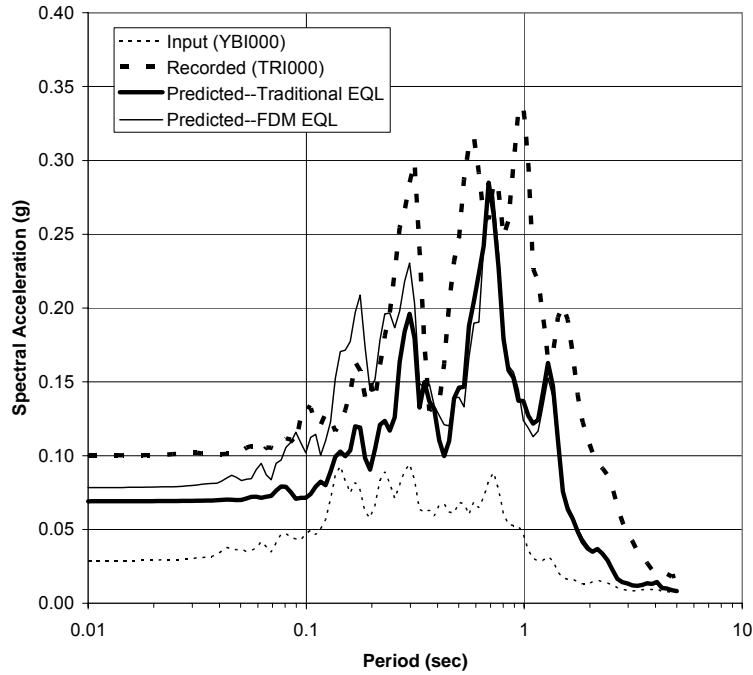


Figure 16. Acceleration response spectra from traditional EQL and FDM EQL site response analysis.

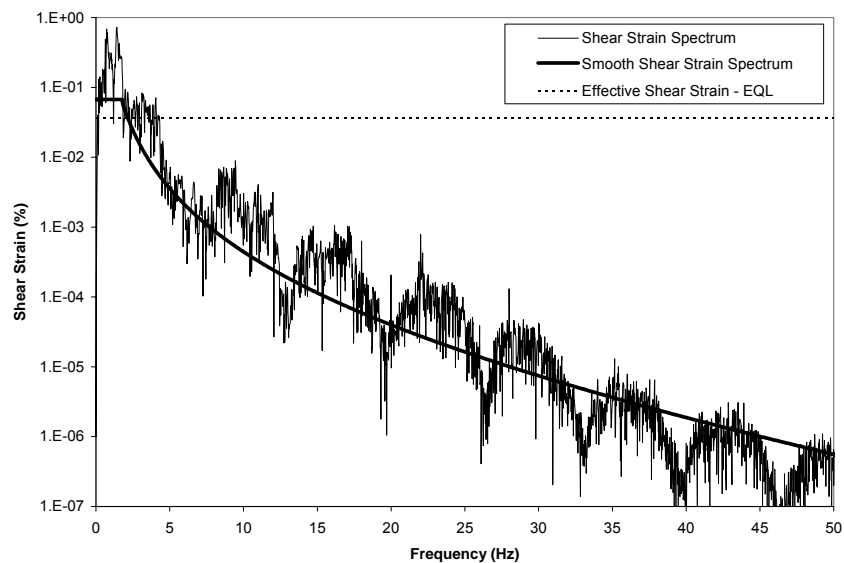
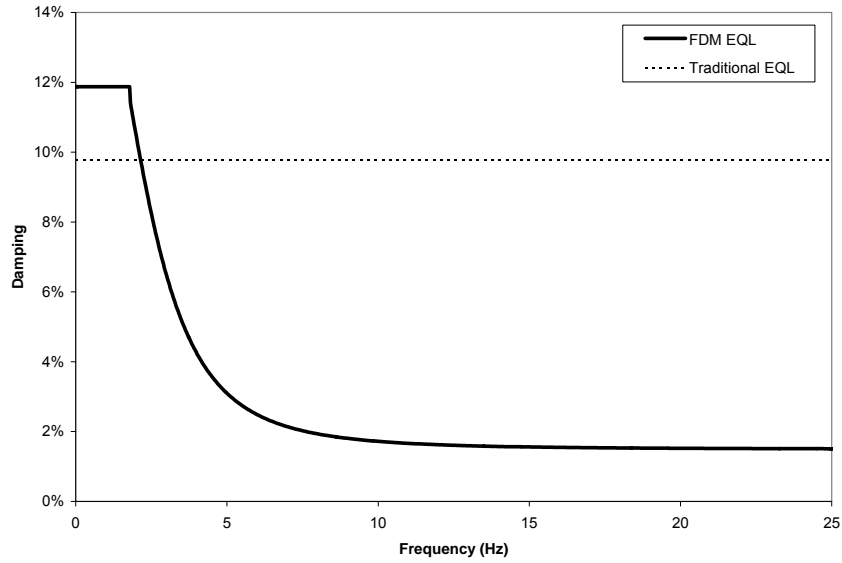
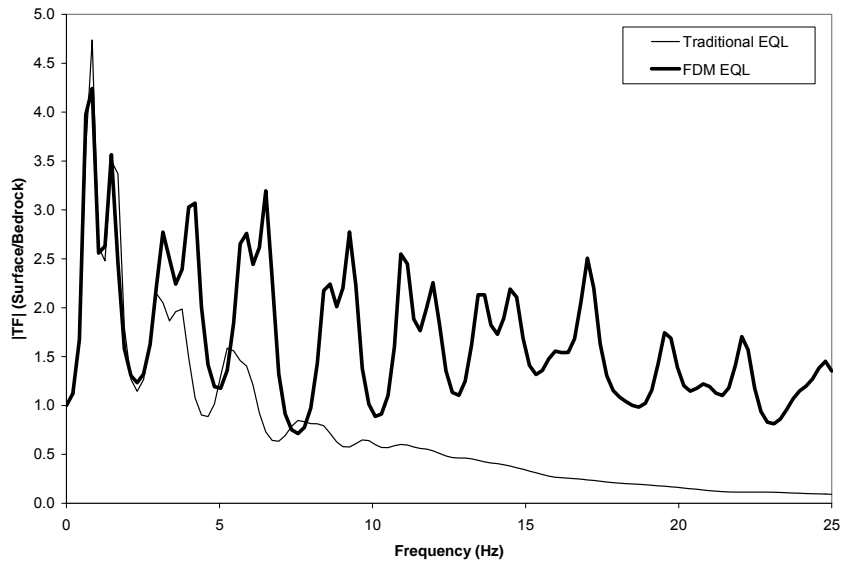


Figure 17. Shear strain spectrum used to define frequency-dependent properties



(a)



(b)

Figure 18. (a) Frequency-dependent damping and (b) transfer functions for traditional and FDM EQL analysis.

damping, the transfer function values are small at frequencies above 5 Hz. For the FDM analysis, the damping at frequencies less than 1.8 Hz is set equal to 12% based on the maximum shear strain computed for the layer. However, the damping is less than 2% at frequencies above about 5 Hz, because of the frequency-dependent shear strain shown in Figure 17. As a result, the higher modes are maintained in the transfer function (Figure 18(b)) and not severely damped out. Thus, higher frequencies are maintained and larger spectral acceleration are predicted at the ground surface (Figure 16).

A final comparison is shown in Figure 19 in terms of the acceleration-time histories at the ground surface predicted by traditional and EQL FDM. Only the most intense part of the record is shown, such that the differences in high frequency content can be emphasized. The larger PGA for the FDM EQL analysis is apparent in Figure 19, but the FDM time series also clearly shows more high frequencies motion on top of the lower frequency motion. As a result, the FDM analysis provides a more realistic looking time history at the ground surface. These differences would be even more apparent at larger intensities (and thus, large strains) and for deeper soil sites.

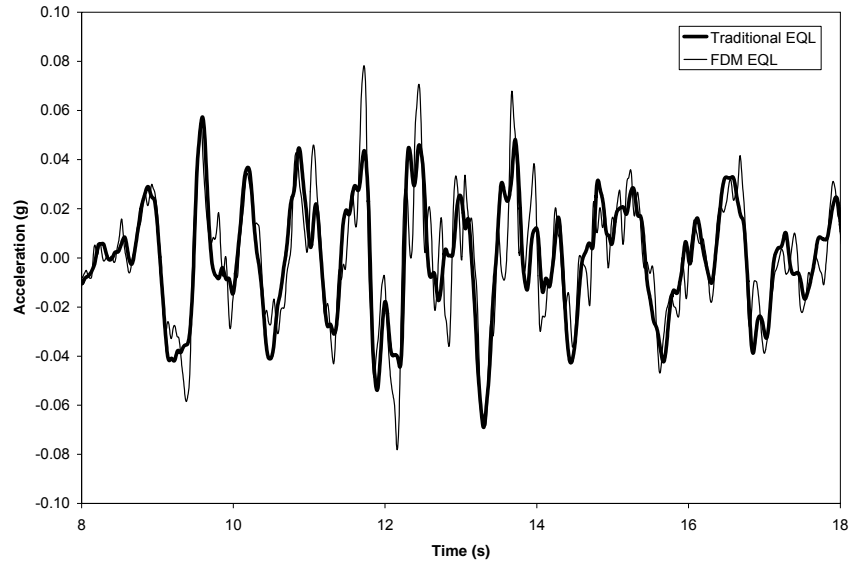


Figure 19. Acceleration-time history at ground surface from traditional and FDM EQL analysis.

CONCLUSIONS

A geotechnical site response module was developed that can be used in the future with OpenSHA or any probabilistic seismic hazard analysis (PSHA) program. The current capabilities of this site response module include RVT-based and traditional EQL site response analysis, as well as FDM EQL site response analysis. RVT analysis is particularly well-suited for PSHA because it predicts the site response without requiring any input time histories. FDM EQL analysis also has a benefit for PSHA. Because the FDM approach does not overdamp high frequencies at large input intensities, it allows EQL analysis to be used for the larger input intensities modeled as part of PSHA.

The site response module was developed in Matlab and used to perform a series of site response calculations for validation. For validation, RVT site response analysis was compared with traditional analysis using time domain input motions. Here, the comparison was favorable, with some slight overprediction of site response by RVT at periods close to the site period. The FDM procedure was implemented and used to predict the surface response at the Treasure Island site in San Francisco, California. In comparison with traditional equivalent-linear procedure, the FDM procedure does not experience overdamping of high frequencies and provides more realistic surface time histories of acceleration.

REFERENCES

- Abrahamson, N. A., and Silva W. J. (1997). "Empirical response spectral attenuation relationships for shallow crustal earthquakes." *Seism. Res. Lett.*, Vol. 68, No. 1, pp. 94-127.
- Atkinson, G. M., and Silva, W. (1997). "An empirical study of earthquake source spectra for California earthquakes." *Bull. Seism. Soc. Am.*, Vol. 87, No. 4, pp. 97-113.
- Beresnev, I.A., and Atkinson, G.M. (1998) "FINSIM: A FORTRAN program for simulating stochastic acceleration time histories from finite faults," *Seismological Research Letters*, 69, pp. 27-32.
- Boore, D. (1983). "Stochastic simulation of high-frequency ground motions based on seismological models of the radiated spectra." *Bull. Seism. Soc. Am.*, Vol. 73, No. 6, pp. 1865-1894.
- Boore, D. M. (2002). "SMSIM: Stochastic Method SIMulation of ground motion from earthquakes." *IASPEI Centennial International Handbook of Earthquake and Engineering Seismology*, Lee, W., Kanamori, K., Jennings, P., Kisslinger, C. Editors, Academic press, Chapter 85.13.
- Boore, D. M. (2003). "Simulation of ground motion using the stochastic method." *Pure Appl. Geophys.*, Vol. 160, No. 3-4, pp. 635-676.
- Boore, D. M., and Joyner, W. B. (1997). "Site amplification for generic rock sites." *Bull. Seism. Soc. Am.*, Vol. 87, No. 2, pp. 327-341.
- Brune, J. (1970). "Tectonic stress and the spectra of seismic shear waves from earthquakes." *Journal of Geophysics Research*, Vol. 75, No. 26, pp. 4997-5009.
- Brune, J. (1971). "Correction." *Journal of Geophysics Research*, Vol. 76, No. 20, pp. 5002.
- Campbell, K. W. (2003). "Prediction of strong ground motion using the hybrid empirical method and its use in the development of ground-motion (attenuation) relationships in Eastern North America." *Bull. Seism. Soc. Am.*, Vol. 93, No. 3, pp.1012-1033.
- Cartwright, D. E., and Longuet-Higgins, M. S. (1956). "The statistical distribution of the maxima of a random function." *Proc. Roy. Soc. London*, Ser. Vol. A237, pp. 212-232.
- Dickenson, S.E. (1994). "The dynamic response of soft and deep cohesive soils during the Loma Prieta earthquake of October 17, 1989," *Ph.D. Dissertation*, Univ. of California, Berkeley.
- EduPro (1998) ProSHAKE User's Manual.
- Electric Power and Research Institute (1993) "Guidelines for Determining Design Basis Ground Motions. Volume 1: Method and Guidelines for Estimate Earthquake Ground Motion in Eastern North America," EPRI TR-102293, Electric Power and Research Institute, Palo Alto, CA.
- Gasparini, D. A., and Vanmarcke, E. H., (1976) *SIMQKE: Simulated earthquake motions compatible with prescribed response spectra*, Mass. Institute of Tech., Cambridge, Massachusetts.
- Hanks, T. and McGuire, R. (1981). "The character of high-frequency strong ground motion." *Bull. Seism. Soc. Am.*, Vol. 71, No. 6, pp. 2071-2095.
- IBC (2003), "International Building Code." by *International Code Council*, Delmar Publishers.
- Idriss, I. M., and Sun, J. I. (1992). *SHAKE91: A Computer Program for Conducting Equivalent Linear Seismic Response Analyses of Horizontally Layered Soil Deposits*, Center for Geotechnical Modeling, Department of Civil and Environmental Engineering, University of California, Davis.
- Kausel, E., and Assimaki, D. (2002) "Seismic simulation of inelastic soil via frequency-dependent moduli and damping," *Journal of Engineering Mechanics*, ASCE, **128(1)**, 34-47.

- Lee, M., and Finn, L. (1991) “DESRA-2C: Dynamic Effective Stress Response Analysis of soil deposits with energy transmitting boundary including assessment of liquefaction potential,” University of British Columbia, Vancouver, Canada.
- Li, S., Wang, Z., and Shen, C. (1992) “SUMDES – A nonlinear procedure for response analysis of horizontally layered sites subjected to multi-directional earthquake loading,” Department of Civil Engineering, University of California, Davis.
- Matasovic, N. and Vucetic, M. (1995) “Seismic response of soil deposits composed of fully-saturated clay and sand layers,” Proc, First International Conference on Earthquake Geotechnical Engineering, Balkema, Vol. 1, Tokyo, Japan, November 1995, pp. 611-616.
- Ozbey, M.C. 2006. *Site Specific Comparisons of Random Vibration Theory-based and Traditional Seismic Site Response Analysis*, Ph.D. Dissertation, University of Texas, Austin, TX.
- Rathje, E.M., Kottke, A.R., and Ozbey, M.C. 2005. “Using Inverse Random Vibration Theory to Develop Input Fourier Amplitude Spectra for Use in Site Response,” *16th International Conference on Soil Mechanics and Geotechnical Engineering: TC4 Earthquake Geotechnical Engineering Satellite Conference*, Osaka, Japan, September, pp. 160-166.
- Rathje, E.M., and Ozbey, M.C. 2006. “Site Specific Validation of Random Vibration Theory-Based Site Response Analysis,” *Journal of Geotechnical and Geoenvironmental Engineering*, ASCE (accepted for publication).
- Schneider, J. F., Silva, W. J., Chiou, S. J., Stepp, J. C. (1991). “Estimation of ground motion at close distances using the band-limited-white-noise model.” Proc., Fourth Int. Conf. on Seismic Zonation, EERI, Stanford, CA, Vol. 4, pp. 187-194.
- Silva, W. J., Abrahamson, N., Toro, G., and Costantino, C. (1997). “Description and validation of the stochastic ground motion model, Final Report.” *Brookhaven National Laboratory*, Contract No. 770573, Associated Universities, Inc. Upton, New York

PUBLICATIONS RESULTING FROM THIS WORK

- Rathje, E.M., Ozbey, M.C., and Kottke, A. 2006. “Site Amplification Predictions Using Random Vibration Theory,” *1st European Conference on Earthquake Engineering and Seismology*, 3-8 September, Geneva, Switzerland.
- Rathje, E.M., and Ozbey, M.C. 2006. “Site Specific Validation of Random Vibration Theory-Based Site Response Analysis,” *Journal of Geotechnical and Geoenvironmental Engineering*, ASCE (accepted for publication).
- Ozbey, M.C. 2006. *Site Specific Comparisons of Random Vibration Theory-based and Traditional Seismic Site Response Analysis*, Ph.D. Dissertation, University of Texas, Austin, TX.
- Rathje, E.M., Kottke, A.R., and Ozbey, M.C. 2005. “Using Inverse Random Vibration Theory to Develop Input Fourier Amplitude Spectra for Use in Site Response,” *16th International Conference on Soil Mechanics and Geotechnical Engineering: TC4 Earthquake Geotechnical Engineering Satellite Conference*, Osaka, Japan, September, pp. 160-166.